Dynamic Model Testing of a Combined C-Gen Magnetic Gear System for an Oscillating Wave Surge Converter

Richard Crozier[#1], Ben McGilton[#2], Markus Mueller[#3]
[#]*Institute for Energy Systems,*
University of Edinburgh,
Scotland, United Kingdom
[1]r.crozier@ed.ac.uk
[2]ben.mcgilton@ed.ac.uk
[3]markus.mueller@ed.ac.uk

***Abstract*—The high operation and maintenance (O&M) costs of wave energy converters are a large impediment to the technology's development. Magnetic gears present a promising development in this area as, operating through contactless torque transfer, suffer considerably less wear than mechanical alternatives. This paper presents the results of a dynamic analysis of a magnetically geared power take off system that has been designed for use with an oscillating wave surge converter. The results provide a deeper understanding of the behaviour of a magnetically geared system in normal and extreme operation. Particular focus is given to the self correcting behaviour of the system when rotor slip occurs.**

***Index Terms*—magnetic gears, wave energy, marine energy**

I. Introduction

A key issue facing the development of wave energy is the low speed, high force nature of the energy source. This has resulted in the use of large direct drive systems, mechanical gears or other intermediary speed step change mechanism such as hydraulics. Each of these options have related issues, however, such as the physical size, efficiency and cost of large direct drive machines, the reliability of mechanical gears operating in high saline environments and the operation and maintenance issues associated with hydraulic systems.

An alternative solution which is receiving increasing interest in the industry is Magnetic Gear (MG) technology. MGs operate through contactless torque (or force) transfer and therefore have greatly reduced wear in comparison to a mechanical gear. Additionally, MGs have greatly reduced lubrication requirements, high efficiency and inherent overload protection due to the rotors being able to slip and realign under extreme condition forces.

This paper proposes combining a concentric type MG with a C-Gen machine [1] as a suitable Power Take Off (PTO) for an Oscillating Wave Surge Converter (OWSC). C-Gen is a novel, air cored generator with a light weight, modular design. The combined system then results in a compact, lightweight, high efficiency PTO which is well adapted to marine energy conversion.

The open source magnetics modeling software, FEMM, is used to design and model the gear and the C-Gen machine for full scale values. The dynamic response of the entire system is then modeled and assessed using the multibody dynamics analysis software MBDyn in order to develop the understanding of the behavior of magnetically geared systems under normal and extreme operating conditions.

The results are then analysed and discussed with a focus on the suitability of the proposed system in it's application in marine wave energy.

II. C-Gen

First introduced in 2008 by Mueller & McDonald the C-Gen [2], Permanent Magnet (PM) machine shows great potential in high torque applications. The air-cored machine uses a c shaped PM (Figs. 1 & 2) rotor structure that greatly reduces the attractive forces meaning that large power levels are achievable without the need for large, heavy support structures. Furthermore the C-Gen design is highly modular. This allows for stator segments to be removed from the machine for maintenance while allowing the rest of the machine to continue operation. These attributes make the technology particularly appealing in marine renewables where issues with O&M, accessibility and availability greatly impact the technologies competitiveness.

III. Magnetic Gear Theory

MG's operate through the contactless transfer of torque between rotors introducing a speed step change while experiencing virtually no wear and have greatly reduced lubrication requirements reducing maintenance frequency. Additionally, MGs have reduced acoustics, an important factor when considering environmental impacts, and each rotor can be hermetically sealed from the other allowing for greater options regarding marinisation.

As the rotors are not physically connected MG's have the ability to "slip" or break connection when excessive force is applied such as in storm conditions. The rotors will then

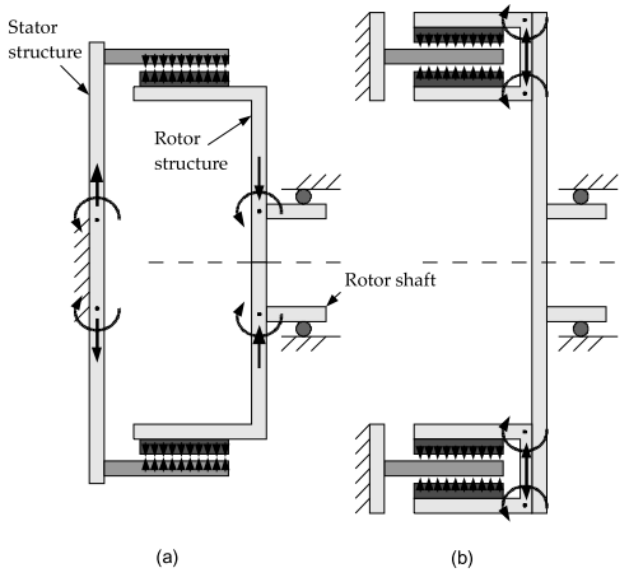

Fig. 1. (a) Conventional permanent magnet radial-flux generator, showing normal forces and their impact on all of the stator and rotor structures (b) C-core machine, showing how normal component of Maxwell stress is isolated within the C- core and does not affect the rotor structure.

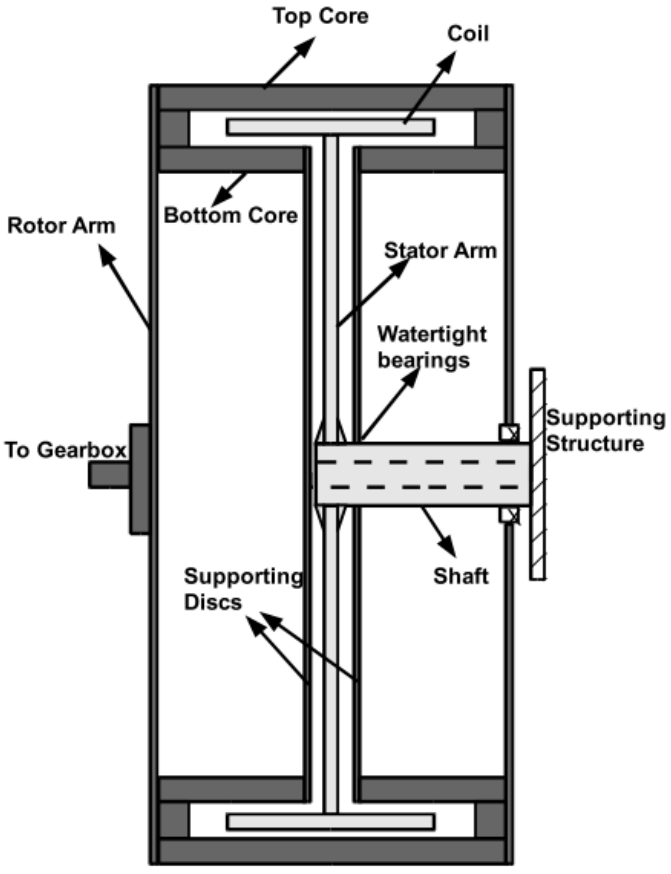

Fig. 2. Rotor and Stator Structure

reconnect when the force is reduced. This grants the MG high levels of survivability which is advantageous given the extreme conditions marine energy converters regularly operate in. MGs are highly adaptable coming in rotary [3], linear [4] and transrotary forms (which convert linear to rotary motion with a velocity increase) [5] and can be utilised with a wide variety of WECs without requiring substantial changes to the generator and without a loss in reliability.

The type of MG designed in this work is a rotary ferromagnetic pole field modulated, Concentric Magnetic Gear (CMG). Though first patented in 1968 [6], it was with Atallah et. al.'s work from 2001 [3] that established its operating principal and high torque capabilities. The CMG is the one of the leading topology in MGs due to it's high torque range which is comparable to mechanical gears (70-150kNm/m^3) and, unlike previous magnetic gear designs, all magnetic material is utilised during torque transfer. This type of MG is realised with the use of ferromagnetic pole (FMP) pieces placed in the airgap between an inner and outer rotor of permanent magnet poles. The FMPs modulate the magnetic field in the airgap such that each rotor sees the corresponding pole number on the opposite rotor allowing for pole alignment and a gearing effect to be established. The gear ratio, G_r, is calculated as:

$$G_r = p_l/p_h = (n_s - p_h)/p_h = -\omega_h/\omega_l \tag{1}$$

Where p_h and p_l are the pole pair numbers on the high and low speed rotors, ω_h and ω_l are the rotational speeds of the high and low speed rotors and n_s is the number of FMP pieces which is determined by:

$$n_s = p_h + p_l \tag{2}$$

Out with these fundamentals there are many parameter related factors which affect the torque ranges of a MG such as magnetic pole height, ferromagnetic pole width and the airgap between rotors. These have been investigated at some length [7]–[11] and are not within the focus of this study. Two primary torque affecting parameters are the airgap radius, which is the distance from the center of the gear to the surface of the inner rotor, and the gear's axial length. These two factors have a dominant effect on the amount of magnetic material in the gears system and therefore the strength of the magnetic field and resulting torque capability. These main elements are shown in Fig. 3).

Pole number can have a large effect on harmonics and can introduce intabilities to a system. To avoid large cogging effects the following equation is used to determine the cogging factor, f_c:

$$f_c = (2pn_s)/(LCM(p, n_s) \tag{3}$$

Where p is the pole pair number on either rotor and LCM is the least common multiple of these two values. For low harmonics this number should be as close to unity as possible.

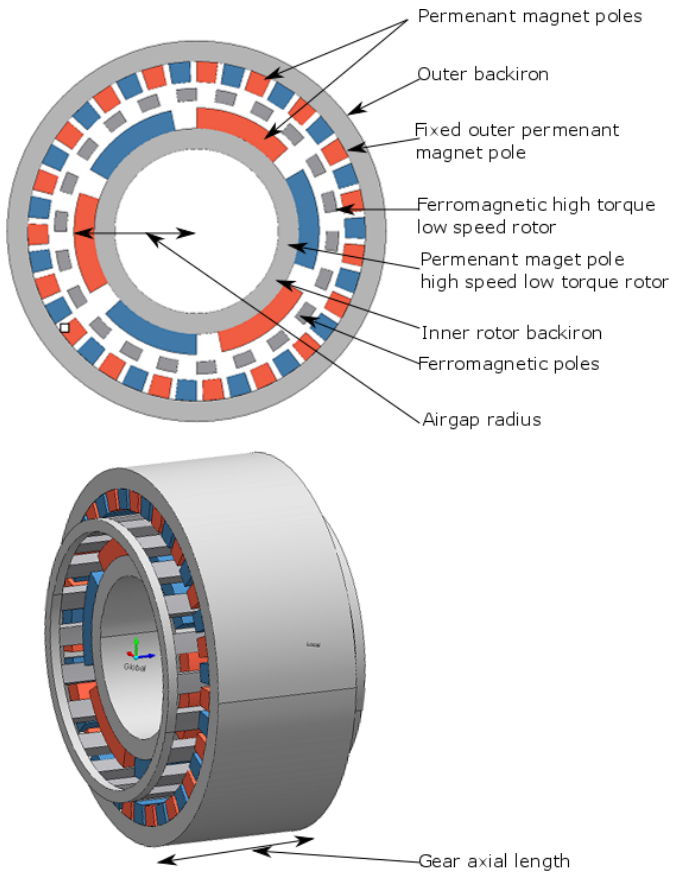

Fig. 3. Main magnetic gear elements.

IV. Case Study

In 2009 Dr. Keysan et. al. produced a study on the application of a C-Gen type electrical machine for the Aquamarine Oyster device PTO (Fig. 4) in place of the hydraulic system then used [1], [12]. The key findings of the report were that due to the low rotational speed (<1rpm) the system would require a single stage gearbox to be feasible. With a gear ratio of between 10-15:1 the efficiency of the generator was around 90% and the total mass was substantially reduced in comparison to a similar direct drive system. The proposed PTO was to place a gearbox-generator system on either side of the devices hinge as shown in Fig. 4. The report further established the torque-speed characteristics of the device finding that having a system capable of 6.2 MNm torque (or two 3.1 MNm, one on each side) would suffice for the device 99.95% of the time and account for 99% of the energy output. As mentioned however, including even a single stage gearbox reduces the advantages of a proposed direct drive system due to the increase in O&M costs associated with mechanical gears. A MG however is theoretically not subject to these high O&M requirements and would allow for a highly efficient system without the additional cost. The MG system developed in this work was for a similar system with two gears developed for 3.1 MNm each and a gear ratio of at least 10:1. The parameters for this model are shown in Table I.

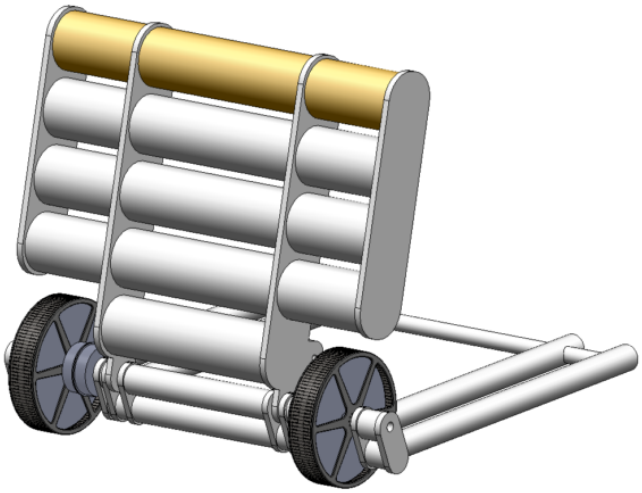

Fig. 4. Aquamarine Oyster Wave Energy Convereter

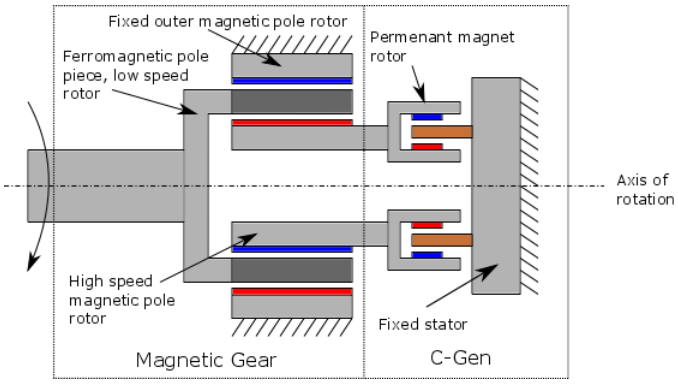

Fig. 5. Gear - Generator topology

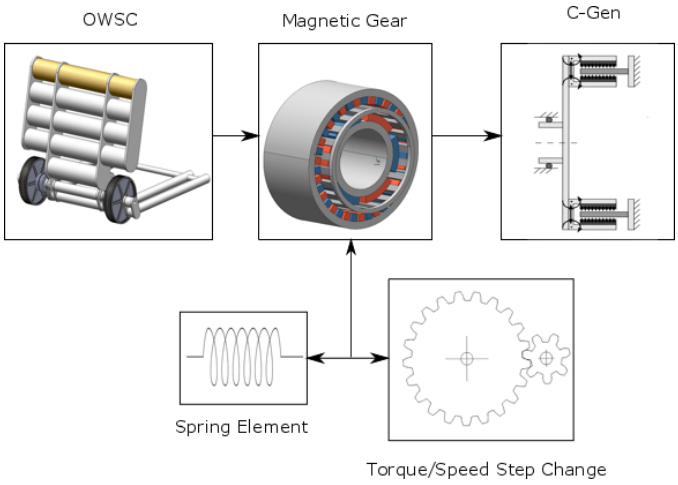

Fig. 6. Full PTO layoput

TABLE I
MG PARAMETER VALUES

Parameter	Value	Unit
Inner magnetic pole thickness	15	mm
Outer magnetic pole thickness	10	mm
Ferro-magnetic pole thickness	20	mm
Airgap radius	1.4	m
Gear axial length	3	m
Inner airgap	1	mm
Outer airgap	1	mm
Outer backiron thickness	20	mm
Inner backiron thickness	20	mm
Outer (fixed) rotor pole pair number	157	
Inner (high speed, low torque) rotor pole pair number	17	
FM (low speed, high torque) rotor pole number	174	
Ratio	10.24:1	
Target high torque	3.1	MNm
Peak (high) torque	3.187	MNm
Peak (low) torque	-0.31198	MNm
Magnetic mass (total)	4224	kg
Active iron mass (total)	10424	kg
Mass of high speed rotor (active)	6576	kg
Mass of low speed rotor (active)	1043.9	kg
Total gear mass (active)	14649	kg

V. DYNAMIC ANALYSIS

MG systems are fundamentally dynamic in nature as, unlike mechanical gears, there will be relative motion between MG rotors. As torque is applied to the high torque rotor the rotor will move as the torque increases on the low torque rotor. The torque development on the gear rotors for the design used is shown in Figs. 7 & 8 while the low speed rotor is held fixed. When the torque is sufficient to overcome the low speed rotor's inertia only then will there be reciprocating motion. A spring effect then occurs whereby the rotor will attempt to catch up with the other rotor while a gearing effect is also observed. As inertia is built on the high speed rotor in the event of a sudden halt in motion there will be some overshoot as the gear attempts to realign to the 0 torque point. [13]

A key point of interest in the dynamic analysis is the "slipping" capabilities of an MG under extreme forces where the peak force is exceeded. In a unidirectional setting this would mean separation of the rotors requiring breaking systems. Given the oscillating nature of a flap device however this dynamic may lend to auto correction. Figs. 5 & 6 show the proposed generator and MG configuration and the full dynamic system being modeled respectively.

VI. MG DYNAMIC MODEL

The dynamic model of the magnetic gear was developed in MBDyn [14], a free multibody dynamics and multiphysics simulation tool with a focus on scientific accuracy, developed for nearly 20 years and first released as an open source tool in 2001. MBDyn uses the concept of "structural nodes" which refer to entities with kinematic degrees of freedom. These nodes can then be constrained with joint elements, have forces or couples applied to them, and masses attached to them.

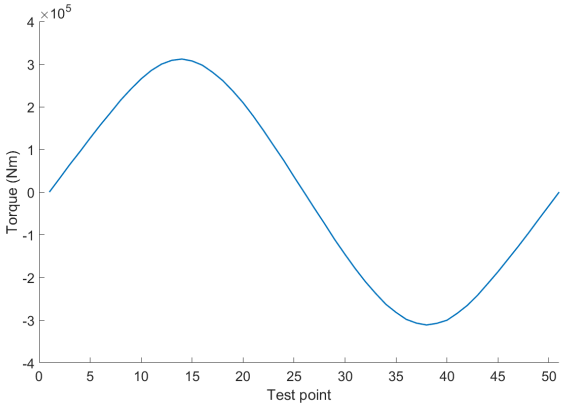

Fig. 7. Torque profile of the high speed, low torque rotor

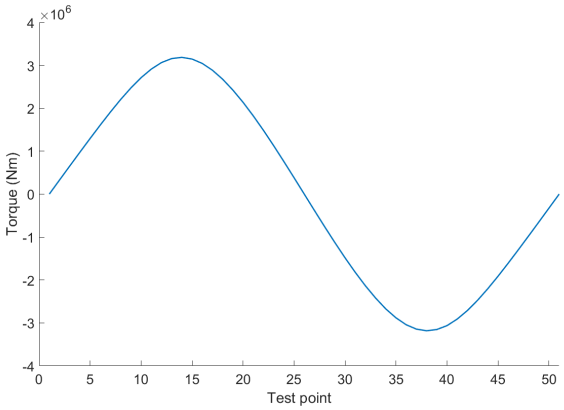

Fig. 8. Torque profile of the low speed, high torque rotor

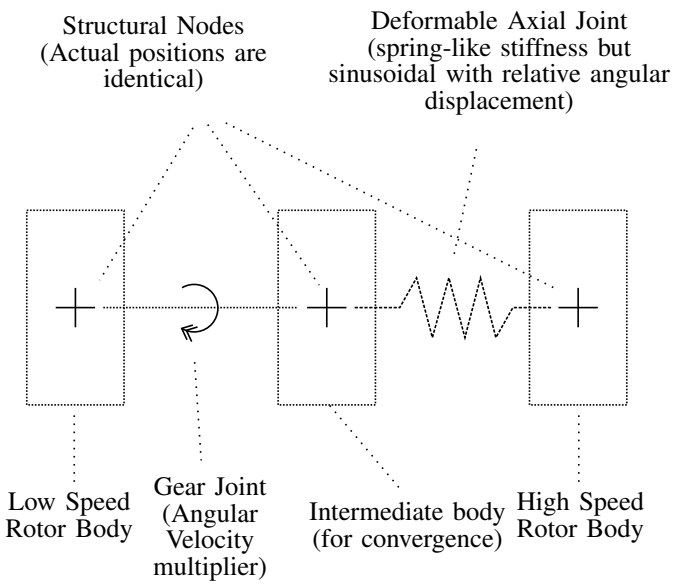

MBDyn provides a very wide range of elements with which to create the multibody system simulation.

In MBDyn, three nodes and five joints are required to model the gear. The first node represents the low speed rotor, while the third node is the low speed rotor. The second node is an intermediate node used to connect the system in the appropriate manner. The first and second nodes, are connected by "Revolute Hinge" joints which constrain the position and orientation of the nodes such than only rotation about a common axis is possible. The second and third node are constrained in the same way. In addition to this, the first and second node are connected by a "Gear Joint" which imposes a relative angular velocity between the two nodes such that the angular velocity of the first node is some multiple of that of the second node. The gear joint element is not available at the time of writing in the official release of MBDyn (which is version 1.7.3). It is a part of the loadable module "module-fabricate" which will be available in a forthcoming release. A preview version of this element was helpfully provided by the developers. To achieve a similar effect to the gear joint, it is also possible to use the "Axial Rotation" joint which imposes an angular velocity on a node about a chosen axis. This angular velocity can be set to be a multiple of the angular velocity of another node. However, the Gear Joint is more reliable and efficient being custom made for this use case.

As shown previously, the cogging force between the rotors is a sinusoidally varying torque with relative displacement of the two rotors. The high speed rotor sees a torque, τ_{HS} which varies as in (4), where θ_{HS} is the angular displacement of the high speed rotor, θ_{LS} is the angular displacement of the low speed rotor, τ_{HSmax} is the maximum cogging torque of the gear.

$$\tau_{HS} = \tau_{HSmax} \sin(p_h(\theta_{HS} - \theta_{LS})) \tag{4}$$

To implement this in MBDyn the "Deformable Axial Joint" was used. The deformable axial joint allows a configuration dependent moment to be applied between two nodes based on their relative rotation about a specified axis. This moment can be defined as a function, which must be differentiable. MBDyn does not yet implement a differentiable sine function and so was modified to add this feature. Three bodies were then attached to the structural nodes. Bodies in MBDyn connect mass and inertia to structural nodes. The low speed rotor body was attached to the first node, and the high speed node to the third node. A very small mass was attached to the intermediate node purely to improve convergence of the solution. A diagram of the multibody system for the gear is shown in Fig. VI where it should be noted that the locations of all structural nodes (and bodies) are coincident, and not displaced as shown in the diagram.

VII. Simulations

A. Simply Driven Gear and Load Model

A fully integrated WEC and PTO model has internal feedback, i.e. the torque applied by the PTO affects the motion of the WEC. For this reason, to demonstrate some properties of the gear dynamic performance in a clear way, some results of a simulation of the gear only, using a very stiff drive are now presented. A simulation was performed with the low speed side of the gear driven in a prescribed sinusoidal motion with an angular velocity amplitude of 0.189 rads^{-1} and period of 8 s. At the same time a damping torque was applied, i.e. where the load torque was given by the formula $\tau_L = -c\omega_{HS}$ with a coefficient, c, of 169 kNs, and where ω_{HS} is the angular velocity of the high speed side of the gear. This damping coefficient was chosen such that the maximum gear transmission torque would be just exceeded as the peak of the sine wave was approached. Although this may seem simplistic, simple linear damping is a common control strategy in the real world WECs which have been implemented. In some cases, active damping, where the coefficient is modified to suit the wave conditions is also used. More advanced control strategies are available, but usually require bi-directional power flow and therefore require significantly more complex systems to implement.

The results of this simulation are presented in Fig. 9. It can be seen that the gear initially tracks the motion of the input drive until the damping torque exceeds the maximum gear torque. At this point, the torque transmission is essentially lost as the gear high speed rotor begins making small (but rapid) oscillations with a low average angular velocity. In this period the net angular displacement does continue to rise slightly, probably due to the gear inertia and neglection of friction. However, as the input drive speed falls from the peak, the gear parts reconnect and the gear begins to again transmit torque and track the input drive motion. This shows that the gear can be used to ride through high torque incidents, and reconnect passively without an advanced control system.

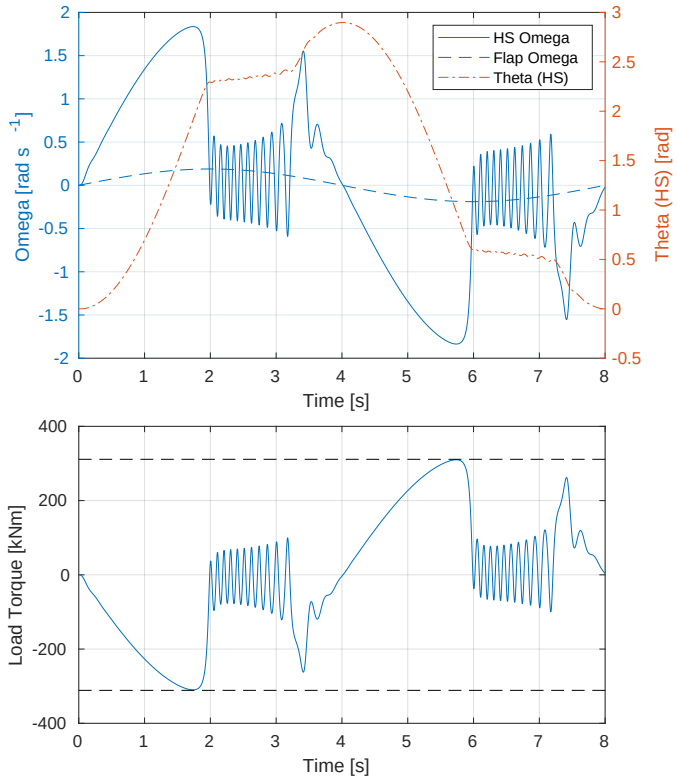

Fig. 9. (top plot) Angular velocities of the Low speed (flap) side of the gear and high speed side, and the angular displacement of the high speed side. (bottom plot) Load torque during simulation (solid line) and max/min gear torques (dashed lines).

B. Gear, Flap and Load Model

To demonstrate that the same basic operation is seen in the full system, a simulation has been performed with the gear operating as part of the drive train of a full OWSC system. The OWSC which will be evaluated is Reference Model 5 (RM5) from the NREL Marine Hydrokinetic Reference Model Project [15]. This model was chosen due its similarity to the Oyster device and the ready availability of the detailed data required for its simulation which has already been validated by experimental tests. Fig. 10 shows a plot of the device, and detailed information on its design may be found in [15].

To simulate the hydrodynamics, a simulation system derived from WEC-Sim [16] was used, the details of which may be found in [17]. This model replaces the use of the Simulink Simscape Multibody with MBDyn for the multibody dynamics calculations, supports multi-rate simulation for different model components and has advanced pre and post-processing capabilities. The development sources of this open-source tool are available online [18], and a version 1.0 release is planned in June 2018. This model consists of two structural nodes and two bodies and was coupled to the previously described magnetic gear model by constraining the rotation of the gear low speed node to be the same as that of the flap node. In the real system two gears would be used and two generators. For the purposes of this simulation, the double gears where modelled

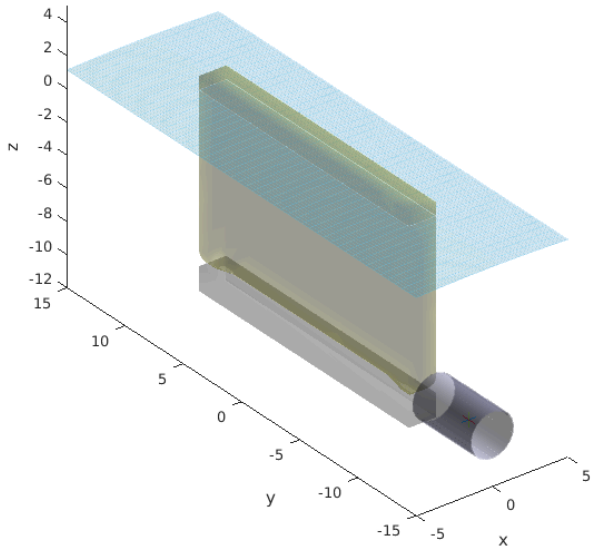

Fig. 10. Diagram of OWSC simulation configuration. Flap is shown in yellow above a fixed base plate, the gear is represented as two annular sections, and the water level is indicated with the blue meshed surface.

by doubling the length of the gear, as the torque in this model scales linearly with length. The mass and inertia matrices were also scaled appropriately. This reduced simulation times by reducing the number of degrees of freedom.

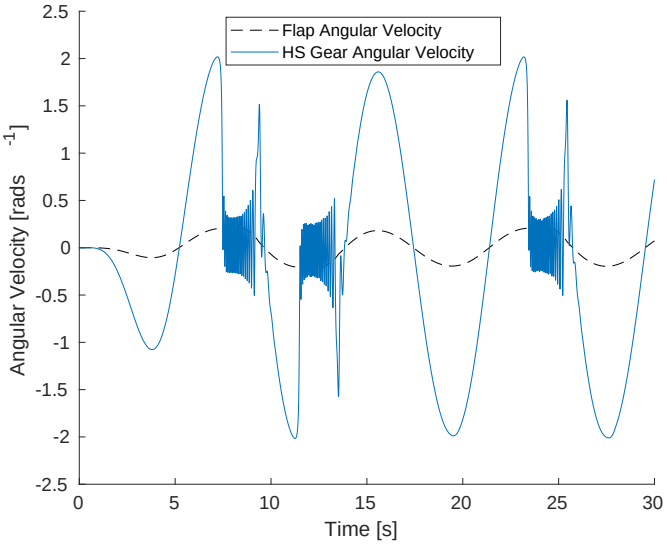

Fig. 11. Angular velocities of the Low speed (flap side) of the MG and high speed side during the OWSC simulation.

The OWSC was simulated with an incoming regular wave, but with an amplitude being increased with a ramp from zero to a peak significant wave height of 2.5 m. The waves have a period of 8 s, and the ramp up in wave height occurs over a 5 second duration. As in the previous simulation, a damping torque which scales linearly with angular velocity was applied, in this case with a damping coefficient of 307.4 kNs (or

153.7 kNs per gear). This value was mainly chosen through trial and error to result in the gear peak torque being just exceeded close to the peak angular velocity of the WEC motion. The resulting angular velocities of the flap and high speed side of the MG are shown in Fig. 11. The applied PTO torque over the same period is shown in Fig. 12.

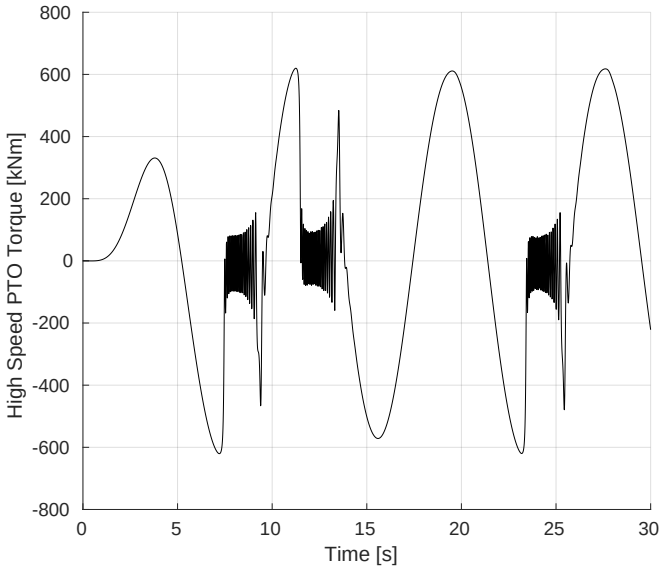

Fig. 12. High speed load torque during the OWSC simulation.

These results show that the results from the simple simulation also hold for the full system simulation, at least in this specific case. The gear connection slips at the peak velocity, but passively reconnects as the wave event progresses. Interestingly, in some cases this seems to impact the system performance in the following wave such that the maximum angular velocity which is achieved is reduced and no slipping occurs.

VIII. Discussion

A much more extensive study in a greater range of wave conditions, especially random waves from a wave spectrum, would be necessary to fully understand the dynamic behaviour of the gear. These preliminary results do though indicate that the gear can offer some additional protection for extreme wave events (or control or PTO failures) where it can act as a kind of filter for extreme torque spikes either side of the gear. The statistical distribution of waves mean extreme events are to be expected, and must be designed for in any system. A magnetic gear interface could facilitate the design of the PTO by providing a limit on the possible peak loading from the prime mover. As the peak loads are one of the main drivers of the design, this could ease significantly the required specifications of the PTO.

The control system used for the PTO here was very basic, a simple damper. It is possible that with a slightly more advanced system, the duration of the slip event could be significantly reduced, and the gear brought back into operation much faster, e.g. by tracking the motion of the flap during the slip event. Similarly one could simply limit the maximum PTO torque on the high speed side to a value less than the maximum MG transmission torque. The gear would still provide protection for failures in the PTO, e.g. a short-circuit fault in the generator, or a control system failure, preventing them from impacting the rest of the system significantly.

There are also possible negative consequences of slip. One is a total loss of control of the device during the slipping period as there is no torque transmission. For some devices, such as a OWSC this is probably not a significant issue, as an undamped OWSC is limited in the deviations it will experience, even in extreme storm conditions. In fact the MG may allow continued power production during such conditions, where previously this was impossible. However, for other types of WEC, this could be a serious issue if the PTO is used to prevent excessive motion.

Another negative aspect of slip, which has not been modelled in this work is that it will likely lead to losses in the MG which do not occur during normal operation. Under slip conditions there is much more relative motion of the various conductive components and the magnetic fields from the magnets. This will result in iron losses and heating in the gear components. Furthermore, the magnetic poles are forced into opposing one another periodically which, together with the heating, will increase the risk of demagnetisation of the magnets. A detailed study of these aspects would be necessary before implementing a system designed to slip under extreme conditions. However, if the design is such that slip events should be rare and short lived, it is likely that any heating should be limited, and the demagnetisation risk can be designed out appropriately.

Although a magnetic gear is likely to be significantly more costly than a conventional gear, it may be the case that the reduced intervention rates required for maintenance, coupled with the inherent overload protection could make it cost-competitive with conventional systems when a holistic view is taken of the system.

IX. Conclusions

Magnetic gears have various features which make them interesting for wave energy developers, the low friction interface has the potential for reducing operation and maintenance costs by reducing intervention rates. They also have the potential to operate mostly flooded, apart from some easily sealed bearing units, which can ease other system requirements, as a C-Gen generator can also potentially operate flooded.

Simulation of the dynamic performance of an MG system during extreme torque events have been presented. It has been shown that in a simple isolated MG simulation with an oscillating drive, the MG can slip and exit the slip condition without any active control intervention. It has then further been shown through a system simulation of an OWSC in regular waves that this behaviour can still be observed.

X. Acknowledgments

The authors would like to acknowledge the support of the U.K Engineering and Physical Science Research Council, EPSRC, for the award of a studentship which is directed through the Wind and Marine Energy, Center for Doctoral Training.

References

[1] O. Keysan, M. Mueller, R. Doherty, M. Hamilton, and A. McDonald, "C-GEN, a lightweight direct drive generator for marine energy converters," *5th IET International Conference on Power Electronics, Machines and Drives (PEMD 2010)*, pp. 244–244, 2010.

[2] M. Mueller and A. McDonald, "C-gen a lightweight permanent magnet generator for direct drive power take off systems," pp. 1–7, 10 2008.

[3] K. Atallah and D. Howe, "A novel high-performance magnetic gear," *IEEE Transactions on Magnetics*, vol. 37, no. 4 I, pp. 2844–2846, 2001.

[4] R. C. Holehouse, K. Atallah, and J. Wang, "Design and Realization of a Linear Magnetic Gear," *Magnetics, IEEE Transactions on*, vol. 47, no. 10, pp. 4171–4174, 2011.

[5] M. B. Kouhshahi and J. Z. Bird, "Analysis of A magnetically geared lead screw," *Electrical and Computer Engineering Faculty Publications and Presentations*, no. 421, pp. 1–8, 2017.

[6] M. B, "Magnetic transmission," Apr. 16 1968, uS Patent 3,378,710. [Online]. Available: http://www.google.co.uk/patents/US3378710

[7] L. Y. L. Yong, X. J. X. Jingwei, P. K. P. Kerong, and L. Y. L. Yongping, "Principle and simulation analysis of a novel structure magnetic gear," *International Conference on Electrical Machines and Systems*, no. 1, pp. 3845–3849, 2008.

[8] N. W. Frank and H. a. Toliyat, "Gearing ratios of a magnetic gear for wind turbines," *2009 IEEE International Electric Machines and Drives Conference, IEMDC '09*, pp. 1224–1230, 2009. [Online]. Available: http://ieeexplore.ieee.org/xpl/login.jsp?tp={\&}arnumber=4906554{\&}url=http://ieeexplore.ieee.org/iel5/4839121/4906480/04906554.pdf?arnumber=4906554

[9] P. O. Rasmussen, T. O. Andersen, F. T. Jørgensen, and O. Nielsen, "Development of a high-performance magnetic gear," *IEEE Transactions on Industry Applications*, vol. 41, no. 3, pp. 764–770, 2005.

[10] T. Lubin, S. Mezani, and A. Rezzoug, "Analytical computation of the magnetic field distribution in a magnetic gear," *IEEE Transactions on Magnetics*, vol. 46, no. 7, pp. 2611–2621, 2010.

[11] Z. Zhu and D. Howe, "Influence of design parameters on cogging torque in permanent magnet machines," *IEEE Transactions on Energy Conversion*, vol. 15, no. 4, pp. 407–412, 2000. [Online]. Available: http://ieeexplore.ieee.org/lpdocs/epic03/wrapper.htm?arnumber=900501

[12] O. Keysan, A. McDonald, and M. Mueller, "Aquamarine power oyster - C-GEN rotary machine design," *Design*, no. June, 2009.

[13] R. G. Montague, C. M. Bingham, and K. Atallah, "Magnetic gear dynamics for servo control," in *Melecon 2010 - 2010 15th IEEE Mediterranean Electrotechnical Conference*, April 2010, pp. 1192–1197.

[14] P. Masarati, M. Morandini, and P. Mantegazza, "An efficient formulation for general-purpose multibody/multiphysics analysis," *Journal of computational and nonlinear dynamics.*, vol. 9, no. 4, 2014.

[15] Y. H. Yu, D. S. Jenne, R. Thresher, A. Copping, S. Geerlofs, and L. A. Hanna, "Reference model 5 (rm5): Oscillating surge wave energy converter," 1 2015.

[16] Wec-sim (wave energy converter simulator). National Renewable Energy Laboratory (NREL) and Sandia National Laboratories (Sandia). [Online]. Available: https://wec-sim.github.io/WEC-Sim/index.html

[17] R. Crozier and M. Mueller, "Development of a multi-rate wave-to-wire modelling tool," in *Proceedings of the 12th European Wave and Tidal Energy Conference (EWTEC)*, 2017.

[18] Renewnet foundry. [Online]. Available: https://sourceforge.net/projects/rnfoundry/wave